Rapid microfluidic perfusion system enables controlling dynamics of intracellular pH regulated by Na^+/H^+ exchanger NHE1

Quang D. Tran*[a1], Yann Bouret†[a1], Xavier Noblin[1], Gisèle Jarretou[2], Laurent Counillon[2], Mallorie Poët‡[2], and Céline Cohen§[1]

[1] *Université Côte d'Azur, CNRS UMR 7010, Institut de Physique de Nice (INPHYNI), 06108 Nice, France*
[2] *Université Côte d'Azur, CNRS UMR 7370, Laboratoire de PhysioMédecine Moléculaire (LP2M), 06107 Nice, France*
[a]*These authors contributed equally to this work.*

Abstract

pH regulation of eukaryotic cells is of crucial importance and influences different mechanisms including chemical kinetics, buffer effects, metabolic activity, membrane transport and cell shape parameters. In this study, we develop a microfluidic system to rapidly and precisely control a continuous flow of ionic chemical species to acutely challenge the intracellular pH regulation mechanisms and confront predictive models. We monitor the intracellular pH dynamics in real-time using pH-sensitive fluorescence imaging and establish a robust mathematical tool to translate the fluorescence signals to pH values. By varying flow rate across the cells and duration for rinsing process, we manage to tweak the dynamics of intracellular pH from a smooth recovery to either an overshooting state, where the pH goes excitedly to a maximum value before decreasing to a plateau, or an undershooting state where the pH is unable to recover to $\sim$7. We believe our findings will provide more insight into intracellular regulatory mechanisms and promote the possibility of exploring cellular behavior in the presence of strong gradients or fast changes in homogeneous conditions.

1 Introduction

Biological processes are nearly all pH dependent, and hence, this is why this parameter is so tightly controlled[1,2]. Quantitatively, pH represents the abundance of the smallest cation in the universe in aqueous solution and is measured as the cologarithm of free H^+ concentration. At the cellular level, pH is both one of the most finely tuned parameters and one of the most challenging to control. Indeed, (i) many reactions result in the rapid release or consumption of protons and/or acid-base equivalents, (ii) respiratory complexes use H^+ gradients across membranes to produce and store energy and (iii) pH determines the protonation state of macromolecules and thereby dictates their surface charge that is key for their interactions. Finally, pH is also involved in the catalytic activity of enzymes that use acid-base catalytic mechanisms and/or is a critical allosteric regulator of enzymes or membrane proteins. There are numerous reviews on pH regulation, which provide invaluable insights in both normal and pathological conditions[3–5].

To achieve the challenge of finely tuning pH evolution in time and space, evolution has selected a large group of proteins capable of transporting acid-base equivalents across membranes. These include pumps[6], leaks and secondary transporters[7–9] that can translocate H^+, bicarbonate[10] or others buffers. In this context, we have previously built a fully tractable mathematical model for pH regulation that in particular predicts overshoots of pH recovery when a transient change that produces an acidification is suddenly removed[11]. Such and important property is biologically important as it could lead to pathological situations if not adequately damped, possibly by functional redundancy.

To challenge such a mechanism in detail, it is crucial to measure intracellular pH at steady state but even more so to be able to measure the dynamics of pH change depending on cellular conditions. The main gold standard technique to get reliable quantitative pH measurements is based on the use of pH sensitive fluorescent probes, whose absorption and/or emission spectra depend on their protonation state[12]. Different measurement methods and devices are based on such pH-dependent spectral properties of probes, for e.g. fluorometers or fluorescence-equipped microplate readers, but one of the most widely used, due to its ability to image single cells, is based on live fluorescence videomicroscopy equipped with high-resolution camera and ad hoc illumination systems[13]. Although videomicroscopy is widely used, it has certain limitations, particularly when measuring pH changes triggered by very transient disturbances, which therefore require rapid kinetics. Paradoxically, the limits do not presently reside in cameras or illumination systems but in the ability to use very rapid perfusion systems that allow extremely fast exposure to solutions and in parallel the elimination of the incubation medium at the same rate. The work presented here allows for the first time to access this valuable information on rapid intracellular pH variations that enables to document the conditions leading to the occurrence of over-

*Present address: Department of Physics, Brandeis University, Waltham, MA 02453
†Email: yann.bouret@univ-cotedazur.fr
‡Email: mallorie.poet@univ-cotedazur.fr
§Email: celine.cohen@univ-cotedazur.fr

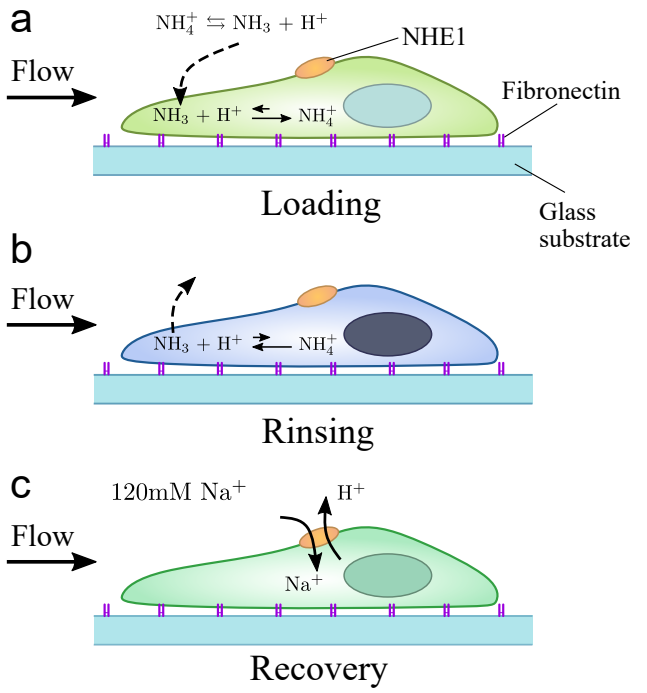

Fig. 1 Schematics of the intracellular pH regulation in 3-step NHE forward activity: a) Loading of NH_4^+ which results in NH_3 entering through cell membrane and absorbing intracellular protons; b) rinsing of NH_3 to release protons inside intracellular region; c) recovery of intracellular pH by exchange of supplied Na^+ ions for intracellular protons through NHE1.

shoots. Actually, the homeostasis of the cell arises from the steady state of competing regulatory phenomenons that are membrane transporters and chemical reactions. In a previous work[11], we proved that alteration of this physiological regulation by a vanishing perturbation - meaning that we start and finish to the exact same experimental parameters - yields a pH overshoot during its relaxation. The dimensions of these overshoots depend on the characteristics of the perturbation that we impose, but neither their amplitude nor their time occurrence obey an analytical expression.

For this study, we developed a laminar flow regime using microfluidics to impose precise and reproducible adequate perturbations in order to quantify their effects on intracellular pH. We performed a 3-step regulation of intracellular pH in a NHE forward activity (Fig. 1), in which protons were extruded from the cytosol to the extracellular environment via a Na^+/H^+ exchanger (NHE1). Our system allowed for rapid perfusion of flow through on-chip cultured cells, featuring real-time monitoring of the intracellular pH. We induced various dynamics of intracellular pH by varying flow rates across the cells or duration for rinsing process, including producing an overshooting state that is challenging to obtain in a traditional perfusion system.

2 Methods and Materials

2.1 Microfluidic design and fabrication

We designed a microfluidic device to feature on-chip cell culture and live imaging (Fig. 2(a)). The device involves a straight microchannel with height of 50 µm, which is separated into 3 regions of different width. Two large regions with 500-µm width for cell culture and observation purposes are placed at two ends of a thin channel (50-µm width) to enhance the hydrodynamic resistance of the channel. The high resistance helps maintain a slow flow of culture medium across the whole channel when there is a slight pressure difference between the inlet and outlet. We selected the single-channel design over the one with multiple inlets as we need to completely remove the dead volume and prevent the solution mixing or diffusion during the pH regulation experiment.

Our microfluidic device was fabricated in PDMS (Sylgard 184, Dow Chemical, Midland, MI, USA) following the standard soft-lithography technique[14–16]. A silicone mold was first obtained by photo-lithography with SU-8 100 (MicroChem, Newton, MA, USA) to deposit the design pattern on a silicon wafer with a desired height of 50 µm. We then produced PDMS chips by mixing PDMS monomers with the curing agent at ratio 10:1 and pouring onto the mold. Being cured after incubation at 70 °C for 2 hours, the PDMS chip was then punched with holes at the inlet and outlet. We sterilized the PDMS chip together with a glass slide by autoclave and then bonded them together using a plasma cleaner (Harrick plasma).

2.2 Surface treatment for on-chip cell culture

Right after the plasma bonding, a fibronectin solution (F1411, Sigma-Aldrich, St. Louis, MO, USA) diluted at 0.1 $mg\,mL^{-1}$ in distilled water was injected into the microfluidic channel. The device was then incubated overnight at room temperature. The fibronectin coating enhances cell adhesion to the device substrate, thus securing cell positions under flow. The coated device needs to be rinsed with PBS and then filled with culture medium in order to be prepared for cell seeding.

2.3 Procedure and reagents for the 3-step NHE forward activity

To facilitate the pH regulation assays for NHE forward activity (Fig. 1), we prepared 3 solutions according to 3 steps: (1) Perfusion of NH_4^+ loading solution (Loading solution in short) consisting of 50 mM NH_4Cl, 70 mM choline chloride, 5 mM KCl, 1 mM $MgCl_2$, 2 mM $CaCl_2$, 5 mM glucose and 15 mM MOPS at pH 7.4. This step results in NH_3 entering cells through the membrane and absorbing H^+ to form NH_4^+. (2) Perfusion of Rinsing solution (120 mM choline chloride, 5 mM KCl, 1 mM $MgCl_2$, 2 mM $CaCl_2$, 5 mM glucose and 15 mM HEPES at pH 7.0), which allow NH_3 to escape and release H^+ inside cells. (3) Perfusion of Recovery solution (120 mM NaCl, 5 mM KCl, 1 mM $MgCl_2$, 2 mM $CaCl_2$, 5 mM glucose

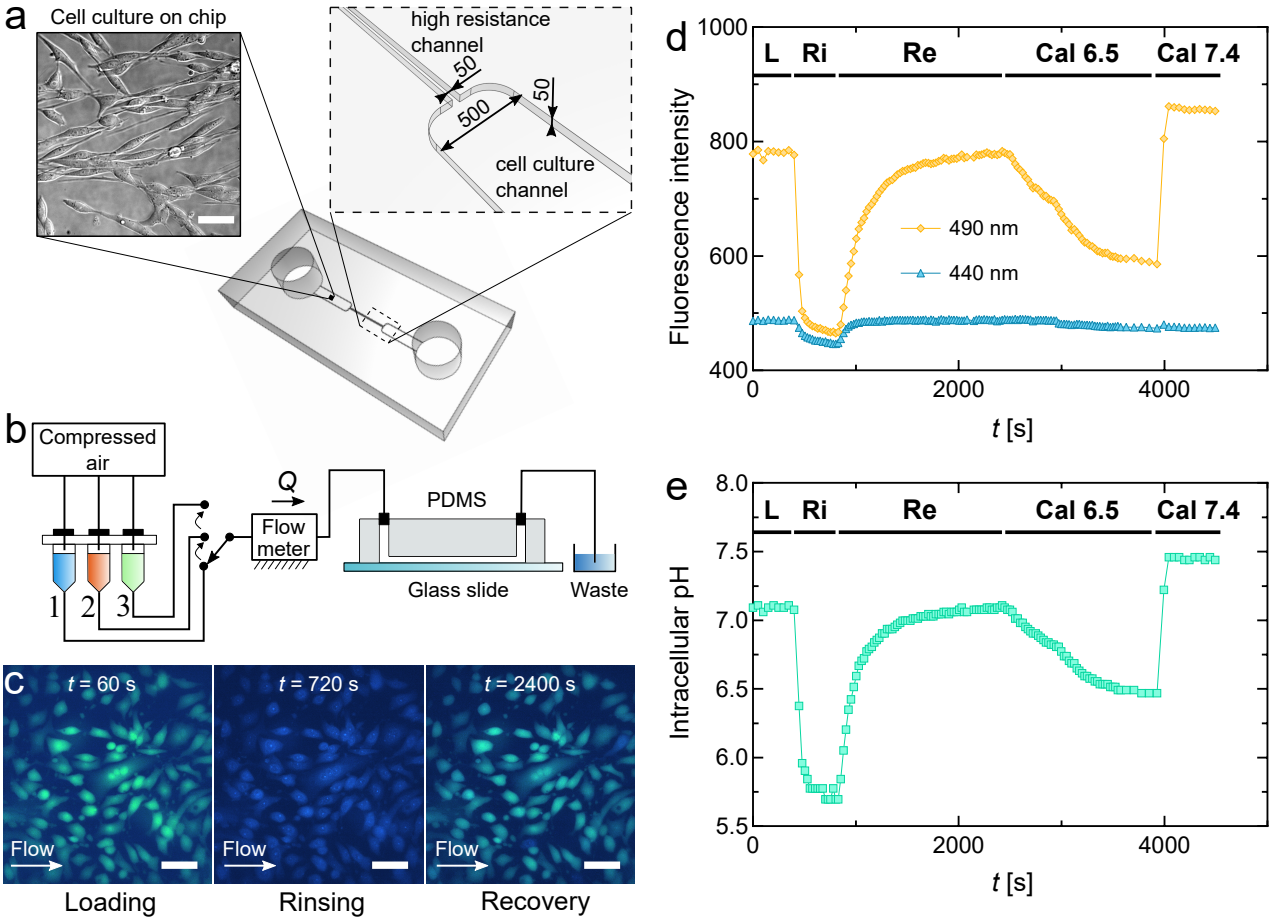

Fig. 2 Experimental setup for intracellular pH measurement. (a) Design of the microfluidic device, which consists of a straight channel with height of 50 μm and 2 cell culture regions ($w = 500$ μm) and a high resistance region ($w = 50$ μm) in between. Cells were cultured on a chip for 2 days. Channel dimensions are in μm. (b) Microfluidic setup for rapid measurement of intracellular pH. Continuous flow was applied to eliminate all dead volumes and unwanted mixtures of solutions. (c) BCECF fluorescent dye was used to quantify the pH values of cells. BCECF-stained cells change color according to their pH levels at different pH regulation activities. Scale bar: 50 μm. (d) Fluorescence intensity of a representative cell from (c) was recorded simultaneously in two wavelengths 490 nm and 440 nm throughout the whole experiment including the Loading, Rinsing, Recovery processes and two calibration processes at pH 6.3 and pH 7.4. (e) Translated intracellular pH values of the representative cell during the whole pH regulation experiment using equation 1. Abbreviations: L – Loading, Ri – Rinsing, Re – Recovery, Cal 6.5 – Calibration pH 6.5, Cal 7.4 – Calibration pH 7.4.

and 15 mM HEPES at pH 7.4), which supplies Na^+ to the system and establishes the H^+ extrusion to extracellular environment via NHE1. At the end of each experiment, we applied two pH calibration solutions consisting of 140 mM KCl, 20 mM HEPES, and 5 μM nigericin with pH values adjusted at 6.47 and 7.44.

2.4 Cell culture, cell suicide and on-chip seeding

In this study, we used PS120 fibroblast cells stably expressing mutant NHE1, a transfected cell line that has been used in our previous studies[11,17,18]. Cells were first cultured in DMEM enriched with 7.5% fetal calf serum and 50 $\mu g\,mL^{-1}$ PenStrep at 37 °C and 5% CO_2. Transfection of NHE1 was performed using Lipofectamin 2000 following the protocol from the manufacturer (ThermoFisher, Waltham, MA, USA).

We performed a cell suicide process, which has been described by Milosavljevic et al.[13] to select and amplify the population of stable NHE1-expressed cells. To summarize, we first incubated the cells for 1 hour in Loading solution at 37 °C inside an incubator without CO_2 supply. Next, we removed the Loading solution and washed the cells twice in the Rinse solution. Finally, we replaced the Rinse solution with Recovery solution and incubated for another 1 hour also without CO_2 supply. CO_2 was not allowed in this process due to the acidification resulting from the interaction between CO_2 and the buffers. The Recovery solution was then aspirated and replaced by fresh culture medium so that the cells continued growing.

Upon cofluent, the cells were trypsinized and suspended in culture medium, then seeded into the microfluidic channel by pipetting. We incubated the microfluidic device containing the cells at 37 °C and 5% CO_2 for 30 minutes. A droplet of fresh culture medium was placed at the inlet of the microfluidic channel, which helped create a continuous flow of fresh medium across the channel and promote cell growth. The high resistance channel is important here as it prevents the droplet

from being rapidly depleted and maintains the slow flow of medium for several days. We cultured the cells inside the microfluidic device for 2 days and refilled the droplet every day.

2.5 Fluorescence pH imaging

To measure the intracellular pH (pH_i), we utilized a ratiometric pH-sensitive fluorescence dye BCECF/AM (B1170, ThermoFisher), which has double excitation and is permeable to cells. The pH measurement was conducted by obtaining the ratio between the emission intensity of the dye when excited at 490 nm and at its isosbestic point of ~440 nm. We stained the cells grown inside the microfluidic device by pipetting 200 μL of BCECF/AM diluted in Loading solution at final concentration of 5 $\mu L\,mL^{-1}$ to the channel inlet. The device was then placed inside an incubator at 37 °C without CO_2 supply for 30 minutes. Before each experiment, we rinsed the microchannel with the Loading solution to remove the excess dye.

2.6 Experimental setup

The microfluidic device containing BCECF-stained cells was connected to our microfluidic system as shown in Fig. 2(a, b). The input flow was applied by a Fluigent pressure control pump (Fluigent, Le Kremlin-Bicêtre, France) integrated with a flow meter, which is able to precisely generate a desired flow rate ranging from 2 to 12 $\mu L\,min^{-1}$. The pressure pump and flow meter were connected to a computer and controlled by MAESFLO software. During experiment, solutions were able to be changed quickly by switching the tubing connectors from one solution to another. The output was connected to an open waste reservoir.

Fluorescence pH imaging of the cells was conducted by an inverted microscope (LEICA DMI6000 B) equipped with 440 nm and 490 nm narrow band interference filters and captured by a high-sensitivity camera (Hamamatsu ORCA-Flash4.0 LT+). Fluorescent cell images and the ratio between emission intensity between 490 nm and 440 nm wavelengths were recorded in real-time using the Leica Application Suite software. The pH regulation was performed by applying a single constant flow rate Q of Loading, Rinsing and Recovery solution across the microfluidic channel, respectively. We started with the Loading process for 10 minutes, then switched to Rinsing for a duration t_r, and finally switch to Recovery. We recorded the data until the fluorescence intensity was stabilized after Recovery. Fig. 2(c) shows images of cells changing their color according to different processes of the pH regulation experiment. At the end of the experiment, we flowed 2 calibration solutions containing nigericin at pH 6.5 and 7.4 into the channel, respectively. We illustrated the acquired data of each experiment in Fig. 2(d).

3 Results and discussion

3.1 Establishment of a rapid microfluidic perfusion system for intracellular pH measurement

We achieved a lab-on-a-chip system for real-time pH_i regulation assays, including cell culture directly inside the device, high precision controllable flow application with different solutions across the cell chamber, and live imaging feature with fluorescence microscopy and versatile data acquisition on multiple cells (Fig. 2). With microfluidics, we were able to fully control the flow rate and exposure time for each pH regulation solution to interact with the cells, which was not possible for previous traditional perfusion systems[13]. By staining the cells with double excitation pH-sensitive fluorescence dye BCECF/AM and using fluorescence microscopy, we captured the cells changing their fluorescence intensity at two different wavelengths (440 and 490 nm) during pH regulation. The software used in the microscopy system (Leica) made it possible to easily select multiple Regions of Interest (ROIs) to record and display data of fluorescence intensity of the two wavelengths in real-time[13]. This helped us observe the behavior of multiple cells and control the flow application according to various experimental purposes.

3.2 Estimation of intracellular pH values directly from fluorescence intensity data

From the ratio of emission intensity between the two wavelengths obtained from the live imaging, the pH_i data of each individual ROI are calculated using the following equation:

$$\mathrm{pH} = \mathrm{p}K + \log\left(\frac{F - \Phi_\alpha}{\Phi_\beta - F}\right) \tag{1}$$

where $\mathrm{p}K \approx 7$ for BCECF/AM, F is the emission intensity ratio measured at each ROI, Φ_α is the intrinsic most acidic ratio of the dye, and Φ_β is the intrinsic most basic ratio of the dye. In this estimation, we need to obtain Φ_α and Φ_β, which requires two ratio values F_a and F_b at two calibration points, one under acidic conditions ($h = h_a$), one under basic conditions ($h = h_b$) with $h = [H^+]$, and both points are far from the experimental zone. With F_a and F_b obtained from experiment, we derive Φ_α and Φ_β from the following equations:

$$\Phi_\alpha = \frac{F_a(K + h_a) - F_b(K + h_b)}{h_a - h_b}, \tag{2}$$

$$\Phi_\beta = \frac{h_a F_b(K + h_b) - h_b F_a(K + h_a)}{K(h_a - h_b)}. \tag{3}$$

Theoretically, there are no values of ratios F that exceed Φ_α or Φ_β, we can apply equation (1) for the hold set of experimental ratios F and the pH value can always be defined (Fig. 2(e)). See Supp. Materials for more details of the calculation.

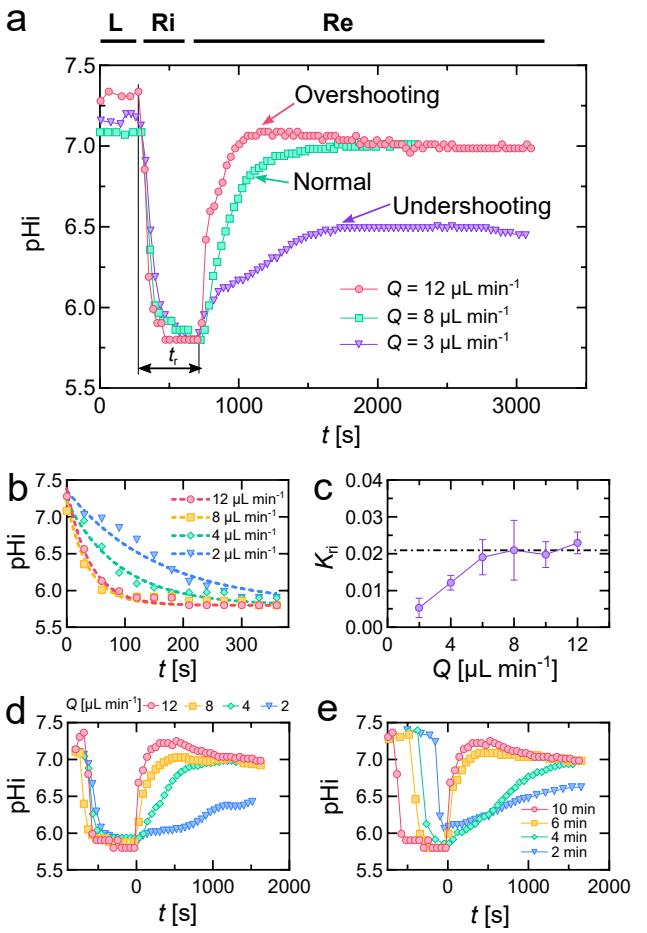

Fig. 3 Behavior of intracellular pH during pH regulation assays. (a) Intracellular pH of representative cells during Loading, Rinsing and Recovery processes with rinsing duration t_r was kept at 6 min and Q varied from 3 to 12 μL min^{-1}. Overshooting phenomenon happened at $Q = 12$ μL min^{-1}, while normal recovery happened at 8 μL min^{-1}, and 3 μL min^{-1} resulted in undershooting. (b) Representative data showing the decay of pH$_i$ over time during Rinsing process at different flow rates. Dashed lines are exponential fits following Eq. 4. (c) The relation between the rinsing reaction rate K_{ri} and Q. Each data point represents the average value from $N = 3$ independent repeats (~20 to 90 cells per condition per repeat). Error bars are standard deviations of the means. (d) Recovery of the intracellular pH of representative cells with rinsing duration $t_r = 10$ min and Q varied from 2 to 12 μL min^{-1}. (e) The effect of rinsing duration t_r on intracellular pH recovery while Q is fixed at 12 μL min^{-1}.

3.3 Different dynamics of intracellular pH observed during the recovery process

We studied the behavior of pH$_i$ of randomly selected cells under different flow rates generated by the pressure pump and flow meter. During the 10 minutes of the Loading process, the pH$_i$ remained stable, then started to drop when the Rinsing solution reached the cells. We first selected the rinsing duration $t_r = 6$ min so that the decreasing pH had enough time to reach a steady state. The Recovery solution was applied at a constant flow rate right after the rinsing duration finished. Interestingly, under different flow rates, the pH$_i$ recovered with different behaviors (Fig. 3(a)). First, we observed that at $Q = 4$ to 8 μL min^{-1}, the pH$_i$ gradually increased to a plateau around 7, which is similar to its common behavior observed in traditional perfusion systems[13]. We name this behavioral state of the pH$_i$ as "Normal recovery." Secondly, for higher Q ($\geq 8\mu$L min^{-1}), the recovery was modified : the pH increased drastically to exceed the intended pH value before decaying and approaching a plateau (Fig. 3(a) and Supp. Movie 1). This pH regulation is called "Overshooting" phenomenon of the pH$_i$. This result confirms the theoretical model introduced by Bouret et al.[11] predicting pH$_i$ can perform overshooting in regulatory loops. However, the overshooting requires a relatively high-speed continuous flow, which might be the reason for this phenomenon to be challenging to obtain in traditional perfusion systems, which apply flow by gravity and do not remove the incubation medium at enough speed that results in some uncontrolled mixing. Finally, when Q was very low ($\leq 3\mu$L min^{-1}), the pH$_i$ recovered very slowly and was not able to reach pH 7, namely "Undershooting" recovery. In many cases of undershooting, the poor pH$_i$ recovery often resulted in cell death. Overall, using microfluidics we have unraveled robustly multiple behavioral states of pH$_i$ recovery in cells under different flow conditions.

3.4 Influence of flow on intracellular pH during rinsing and recovery processes

As the pH$_i$ dynamics were changed according to different flow rates, we investigated how the flow rate affect the kinetics of pH$_i$ during rinsing and recovery process separately. For the Rinsing process, H^+ is released in the cell as NH_3 escapes through the cell membrane (Fig. 1(b)). By applying different flow rates during the Rinsing, we observed the pH$_i$ decrease to a plateau at different rates (Fig. 3(b)). The reaction rate K_{ri} was obtained by fitting the decay of pH value with a single exponential, following the equation

$$[H^+](t) = [H^+]_{eq} + ([H^+]_0 - [H^+]_{eq})e^{-K_{ri}t}. \quad (4)$$

We achieved an increase of K_{ri} with higher rinsing flow rates, but the rate became saturated as $Q \geq 6$ μL min^{-1} (Fig. 3(c)), with the value at saturation $K_{ri} \approx 0.021 \pm 0.001$s^{-1} (mean $\pm$ SD, $N = 3$ repeats). Since the rate of H^+ released in the cell depends on the rate of NH_3 diffusing through the cell membrane, we believe that the system reached a diffusion limit of NH_3 when the flow rate is high enough.

On the other hand, we applied different flow rates during the Recovery process while keeping the rinsing duration at 10 min and monitored pH$_i$ recovery (Fig. 3(d)). The long duration of the rinsing was applied to ensure that the rinsing had reached a steady state before the recovery process. Here, we observed the undershooting occurring at low flow rate (2 μL min^{-1}). At higher flow rates, pH$_i$ turned to the normal recovery and the overshooting state (Fig. 3(d)). We showed that flow rate plays an important role in the recovery dynamics of pH$_i$. In fact, protons extruded by NHE1 result in a local increase in the concentration of proton outside of the cells,

while Na^+ local concentration outside of the cells decreases[19]. This leads to competitive inhibition, as protons can compete with Na^+ for binding to NHE1, which lowers the exchange activity of NHE1[19,20]. Thus, fast flow rates in our microfluidic system help prevent this competitive inhibition and exhibit overshooting behavior of pH_i.

3.5 Rinsing of NH_3 plays a big impact on pH recovery process

To elucidate how rinsing duration affects the recovery of pH_i, we applied a constant flow rate of $Q = 12\ \mu L\,min^{-1}$ with different rinsing duration, from 2 to 10 minutes. We obtained different pH_i recovery behaviors according to different values of t_r. At $t_r = 2$ min, when the rinsing process did not reach the steady state yet, the pH_i recovery experienced a behavior similar to the undershooting state. When $t_r = 4$ min, the pH_i performed normal recovery. At higher rinsing duration ($t_r \geq 6$ min), the pH_i recovered with overshooting behavior at high flow rate $Q = 12\ \mu L\,min^{-1}$. We notice that when the rinsing process is not complete, NH_3 remaining in cells can pick up protons to form NH_4^+. As a result, it affects intracellular proton concentration, which might slow down the recovery dynamics. In addition, we find that the duration of the rinsing should not be longer than 10 minutes, as cells that stay in acidic condition for a long time will become fatal.

3.6 State diagram of intracellular pH recovery

We performed a series of experiments with t_r ranging from 2 to 10 min, and Q ranging from 2 to 12 $\mu L\,min^{-1}$ to map a state diagram for pH_i recovery (Fig. 4). Here, we applied the same flow rate for the rinsing and recovery processes. We observed that low rinsing duration or low flow rates have the same effect on pH_i recovery, which resulted in undershooting state. High flow rates and enough rinsing duration helped the pH_i recover normally or turn to an excited state with overshooting behavior.

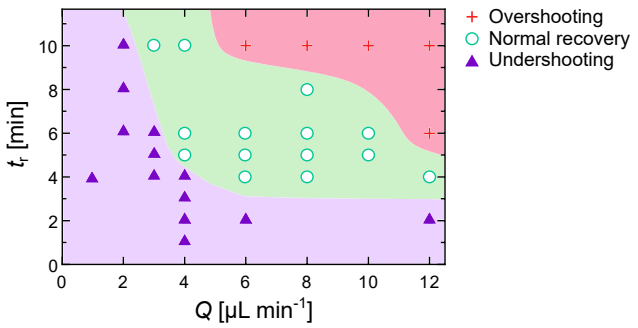

Fig. 4 State diagram of the intracellular pH recovery under different flow rates Q and rinsing duration t_r.

Conclusion

In this study, we have developed a rapid microfluidic perfusion system for intracellular pH regulation assays on cells cultured on-chip. The system featured precise flow rate control of different solutions corresponding to different processes of pH changes and regulation (Loading, Rinsing, Recovery processes) across the cell region, together with live imaging by fluorescence microscopy and real-time data acquisition. We used pH-sensitive fluorescence dye BCECF/AM with double excitations for cell staining to probe pH_i changes over time. We also established a calculation tool to translate the ratios of fluorescence intensity emitted from the two wavelengths of the dye into the pH values in cells. By varying the flow rates of pH regulation solutions and the rinsing durations, we were able to induce a dynamic transition of the intracellular pH, from normal recovery to an overshooting or undershooting state. We also unraveled that the speed of intracellular pH change during the Rinsing process is capped at a limit despite increasing flow rate, which led to our observation that the speed of NH_3 diffusing through the cell membrane is restricted. On the other hand, the recovery speed of intracellular pH, which is governed by the Na^+/H^+ exchanger NHE1, increases as the flow rate increases. If the flow rate is too low, the protons extruded by NHE1 will competitively inhibit NHE1 activity and in the meantime, local Na^+ extracellular concentration will decrease. Fast flow rates allowed by our on chip microfluidic device allow overcome such inhibitory effects and reveal overshooting that is challenging to produce otherwise. Altogether, we provided a robust platform for intracellular pH regulation, which can be further developed to monitor the intracellular pH in real time of complex cellular activities, such as cancer cells during migration or cells exposed to strong gradients and fast changes conditions.

Author contributions

Quang D. Tran: Writing – original draft, Visualization, Validation, Methodology, Investigation, Formal analysis, Conceptualization. **Yann Bouret**: Writing – review & editing, Validation, Project administration, Methodology, Investigation, Formal analysis, Funding acquisition. **Xavier Noblin**: Validation, Supervision, Project administration, Methodology, Investigation, Funding acquisition. **Gisèle Jarretou**: Validation, Methodology, Investigation. **Laurent Counillon**: Validation, Supervision, Project administration, Methodology, Investigation, Funding acquisition. **Mallorie Poët**: Writing – original draft, Validation, Supervision, Project administration, Methodology, Investigation, Funding acquisition, Conceptualization. **Céline Cohen**: Writing – review & editing, Validation, Supervision, Project administration, Methodology, Investigation, Funding acquisition, Formal analysis, Conceptualization.

Conflicts of interest

There are no conflicts to declare.

Acknowledgements

We are thankful for the financial support from IDEX UCA JEDI (ANR-15-IDEX-0001, Nice, France): both from Academie IV (Project MpH) and Structuring Program BOOST (Project COMOZOO), Cancéropole PACA and Université Côte d'Azur. We thank Carina Krahé and Tom Montagnon for their preliminary experiments. We thank Michael Stehnach for fruitful discussions.

References

[1] P. Chan and J. Warwicker, *BMC Biol.*, 2009, **7**, 1–10.

[2] D. Doyen, M. Poët, G. Jarretou, D. F. Pisani, M. Tauc, M. Cougnon, M. Argentina, Y. Bouret and L. Counillon, *Front. Mol. Biosci.*, 2022, **9**, 825028.

[3] J. R. Casey, S. Grinstein and J. Orlowski, *Nat. Rev. Mol. Cell Biol.*, 2010, **11**, 50–61.

[4] M. D. Parker and W. F. Boron, *Physiol. Rev.*, 2013, **93**, 803–959.

[5] M. G. Rolver and S. F. Pedersen, *Brit. J. Cancer*, 2021, **124**, 1–2.

[6] A. F. Eaton, M. Merkulova and D. Brown, *Am. J. Physiol. Cell Physiol.*, 2021, **320**, C392–C414.

[7] S. Pedersen and L. Counillon, *Physiol. Rev.*, 2019.

[8] D. E. Smith, B. Clémençon and M. A. Hediger, *Mol. Aspects Med.*, 2013, **34**, 323–336.

[9] V. Ganapathy and F. H. Leibach, *Curr. Opin. Cell Biol.*, 1991, **3**, 695–701.

[10] W. F. Boron, *J. Pancreas*, 2001, **2**, 176–181.

[11] Y. Bouret, M. Argentina and L. Counillon, *PLoS One*, 2014, **9**, e85449.

[12] F. B. Loiselle and J. R. Casey, in *Measurement of Intracellular pH*, ed. Q. Yan, Humana Press, Totowa, NJ, 2010, pp. 311–331.

[13] N. Milosavljevic, M. Poët, M. Monet, E. Birgy-Barelli, I. Léna and L. Counillon, *J. Vis. Exp.*, 2015, e52453.

[14] G. M. Whitesides, E. Ostuni, S. Takayama, X. Jiang and D. E. Ingber, *Annu. Rev. Biomed. Eng.*, 2001, **3**, 335–373.

[15] Q. D. Tran, D. Gonzalez-Rodriguez *et al.*, *Soft Matter*, 2018, **14**, 6386–6392.

[16] Q. D. Tran, M. Marcos and D. Gonzalez-Rodriguez, *Biomicrofluidics*, 2019, **13**, 054107.

[17] J. Pouysségur, C. Sardet, A. Franchi, G. L'Allemain and S. Paris, *Proc. Natl. Acad. Sci.*, 1984, **81**, 4833–4837.

[18] M. Monet, M. Poët, S. Tauzin, A. Fouqué, A. Cophignon, D. Lagadic-Gossmann, P. Vacher, P. Legembre and L. Counillon, *Sci. Rep.*, 2016, **6**, 28008.

[19] Y. Dong, Y. Gao, A. Ilie, D. Kim, A. Boucher, B. Li, X. C. Zhang, J. Orlowski and Y. Zhao, *Nat. Commun.*, 2021, **12**, 3474.

[20] S. Harguindey, J. L. Arranz, J. D. Polo Orozco, C. Rauch, S. Fais, R. A. Cardone and S. J. Reshkin, *J. Transl. Med.*, 2013, **11**, 1–17.